ELSEVIER

0958-9465(95)00034-8

Cement & Concrete Composites **18** (1996) 3–8

0958-9465/96/$15.00

Analysis of Steel Fibre Pull-Out from a Cement Matrix Using Video Photography

A. Pompo, P. R. Stupak,* L. Nicolais & B. Marchese

Department of Materials and Production Engineering, University of Naples, P.le Tecchio 80, 80125 Naples, Italy

(Received 16 March 1995; accepted 27 June 1995)

Abstract

Video photography of specially prepared specimens allowed identification of the operative energy dissipation mechanisms during pull-out of straight and bent steel fibres from a cement matrix. Correlation between the observed pull-out process and the significant features of the load–displacement curve was established. Both the straight and the bent fibres exhibited fibre/matrix debonding and frictional sliding, while only the bent fibres experienced plastic deformation as an additional energy dissipation mechanism. Qualitative mechanics models explained the dependence of the maximum pull-out and plateau loads as a function of plastic deformation and frictional sliding. Experimentally obtained maximum and plateau loads plotted as a function of fibre diameter squared yielded straight lines that passed through the origin and increased in slope with increasing bend angle.

Key words: Pull-out, steel fibres, bent fibres, energy dissipation, debonding, friction, plastic deformation, video photography.

INTRODUCTION

Brittle materials, when loaded, can absorb little deformational energy before failure. Their toughness can be improved by using short, randomly distributed fibres in the matrix. A fibre in the path of a propagating crack bridges the crack opening and resists further crack growth by dissipating energy during pull-out.[1–4] Steel fibres with different shapes and smooth or irregular surfaces are commercially available[5] and are frequently used to reinforce cementitious matrices. The increased surface roughness and deformed fibre shape results in improved fibre/matrix interaction and gives greater energy dissipation both in the service environment and pull-out tests.[5–13]

A pull-out test of a single fibre embedded in a cementitious matrix is a convenient test to simulate the withdrawal of a bridging fibre and to identify the operative energy dissipation mechanisms.[6,7,12–14] The dissipated energy is equal to the area beneath the load–displacement curve.

It is generally agreed that fibre/matrix debonding and frictional sliding are the two main mechanisms controlling pull-out for a straight fibre. Whereas, not many studies are found in the literature describing the mechanisms active during pull-out of a fibre with a different geometry and surface treatment possibly because of the difficulty of observing the process occurring within the matrix. Some authors[15–17] have used transparent polymeric matrices whose behaviour is substantially different from the brittle cement/fibre interfacial zone and bulk, while some others[18,19] have observed the duct in the matrix after the test using micrography for a better understanding of the process.

The objective of this study was to investigate the energy dissipation mechanisms active during pull-out of steel fibres from cement matrices by video photography of specially prepared specimens. The complete load–displacement curves were described using the digitised images of the photographed fibre pull-out. The main features of the pull-out curve were qualitative related to

*Present Address: SpecTran Corporation, 50 Hall Road, Sturbridge MA 01566 USA.

the main energy dissipation mechanisms, and the experimental maximum and plateau load values showed a linear dependence from fibre diameter squared that increased in slope with increasing bend angle.

EXPERIMENTAL

Hooked steel fibres, Type Dramix ZC 50/0·5, ZC 60/0·8 and ZC 60/1·0 from Bekaert Co., with different aspect ratios, were used. They were warm-water washed and cleaned with acetone to remove any residual polymer binder. The manufactured hook was cut off of one end of the fibre to obtain either straight or intentionally bent fibres. Bend angles were chosen between 0 and 90 degrees with respect to the loading direction during pull-out. The total fibre embedded length was 21 mm and the bent length was 4 mm with diameter of 0·5, 0·8 and 1·0 mm.

Specimens $40 \times 40 \times 160$ mm of Ordinary Portland Cement (OPC) Type I, water/cement ratio of 0·5 by mass, were horizontally cast with embedded fibres perpendicular to the casting direction. After 24 h at 100% humidity, samples were demolded and cured in water for 7, 28 and 90 days.

Samples observed with the video camera were specially prepared by fracture curing, conventionally prepared specimens, so that the flat fracture surface intersected the plane of the embedded fibre. A square glass plate was then adhered to the cement surface to constrain the fibre from out-of-plane motion during pull-out, while allowing a clear view of the process. Most of the lateral surface of the fibre was embedded in the cement, while only a small area was in contact with the glass. Pull-out tests of both the special and conventional samples were conducted using an Instron testing machine with a 10 mm/min crosshead speed.

RESULTS

A characteristic load–displacement (P–Δ) curve obtained for a conventionally prepared straight fibre specimen is represented in Fig. 1 where a linear elastic region is followed by debond crack growth along the fibre/matrix interface at load P_d. After having reached a maximum, the load decreases rapidly at first and then nearly linearly approaching zero load where there is a small sudden drop to zero as the fibre is pulled out of the sample. Therefore, for the straight fibre, only the debond process and the small frictional sliding force after debonding contribute to the energy dissipation during pull-out. The pull-out process of bent fibres is more complex (Fig. 2). The specially prepared samples containing different fibre diameters and bend angles of 33° and 90° were photographed with a video camera during pull-out to gain understanding of the entire process.

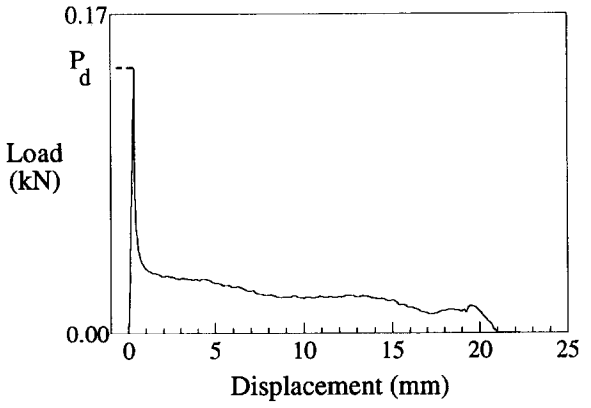

Fig. 1. Experimental pull-out load vs displacement results for a conventionally prepared sample with a 1·0 mm diameter straight fibre after 90 days of water curing.

The load–displacement curves obtained with the special samples reproduced the important features of the conventional pull-out specimens. Only the load values were slightly lower and the data scatter somewhat increased (Fig. 3).

By viewing the video recording of the pull-out event and calculating the corresponding fibre displacement from the recording time, it was possible to correlate the operative energy dis-

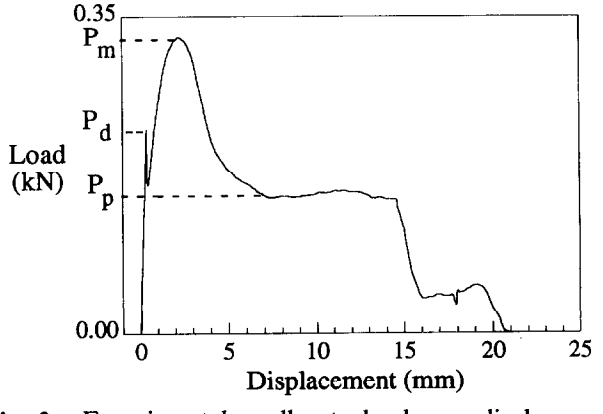

Fig. 2. Experimental pull-out load vs displacement results for a conventionally prepared sample with a 1·0 mm diameter fibre and bend angle of 23° after 90 days of water curing.

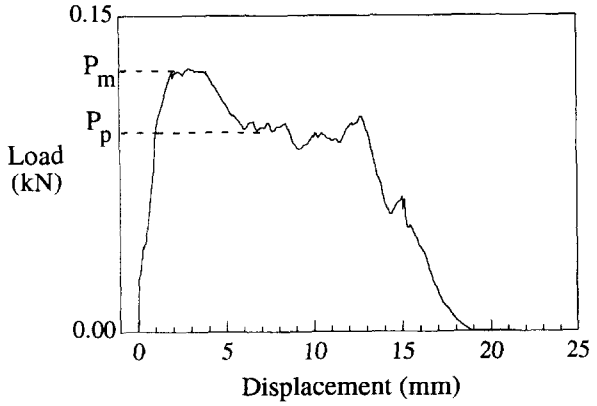

Fig. 3. Experimental pull-out load vs displacement result for a specially prepared sample with a 1·0 mm diameter fibre and bend angle of 33° after 7 days of water curing. The main features of a conventionally prepared sample (i.e., P_m and P_d) are reproduced qualitatively.

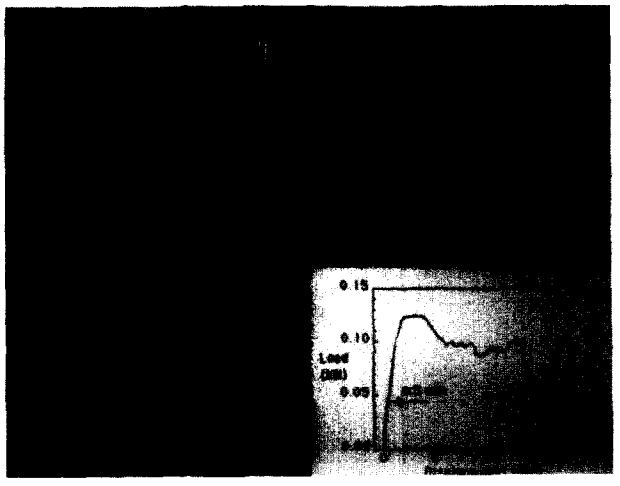

Fig. 5. Digitised image of the same sample at 3 s after test initiation. The corresponding displacement is indicated by an arrow.

sipation mechanisms of the pull-out process with the significant features of the experimental load–displacement curve.

Figure 4 shows the digitised image taken prior to the test for the same sample shown in Fig. 3.

In Fig. 5 the sample is shown 3 s after the test initiation corresponding to a displacement of 0·5 mm on the pull-out curve. Fractured zones (A) and (B) show the areas where the contact stress between the fibre and the matrix walls was greatest. At this point the fibre had already debonded (P_d) and had begun to slide from its original position.

Figure 6 shows the fibre at 4 mm displacement where the fibre tip is aligned with the straight part of the cement duct in the matrix. Up to this point the fibre was plastically deforming and also causing some crushing of the cement matrix near the bend in the matrix duct. It is important to note that the plastic deformation of the fibre was confined entirely to the original fibre bend.

After 4 mm displacement the plastic deformation of the fibre was completed and the only remaining energy dissipation mechanism was frictional sliding of the still partially bent fibre within the straight matrix duct. Because of some residual deformation, the fibre contacted the duct wall at three points indicated by white arrows in Fig. 7. The corresponding region on the load–displacement curve was a plateau where the average load was nearly constant.

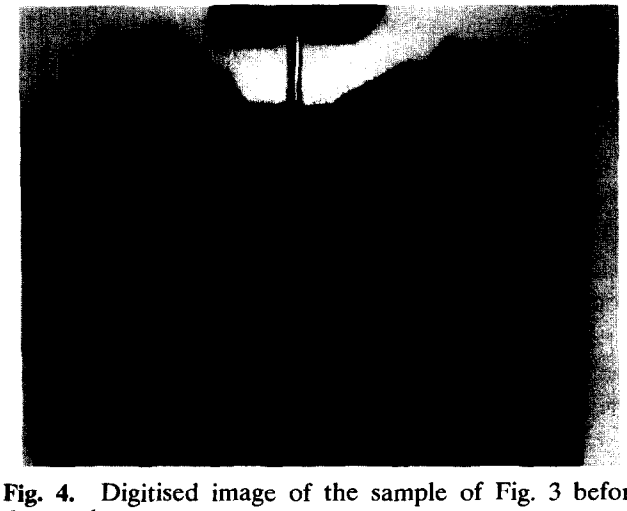

Fig. 4. Digitised image of the sample of Fig. 3 before the test began.

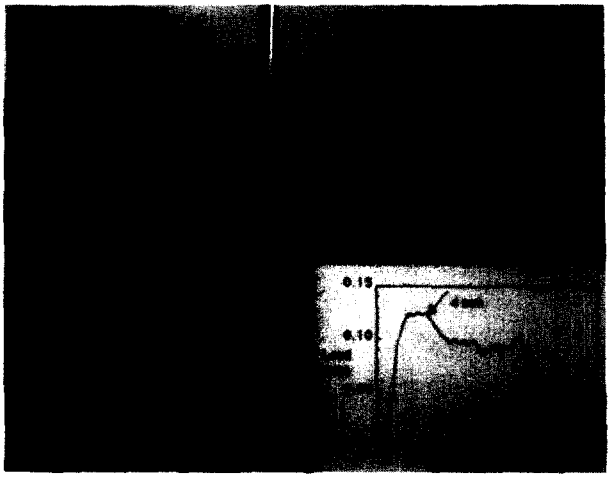

Fig. 6. Digitised image of the same sample at 24 s after test initiation. The corresponding displacement is indicated by an arrow.

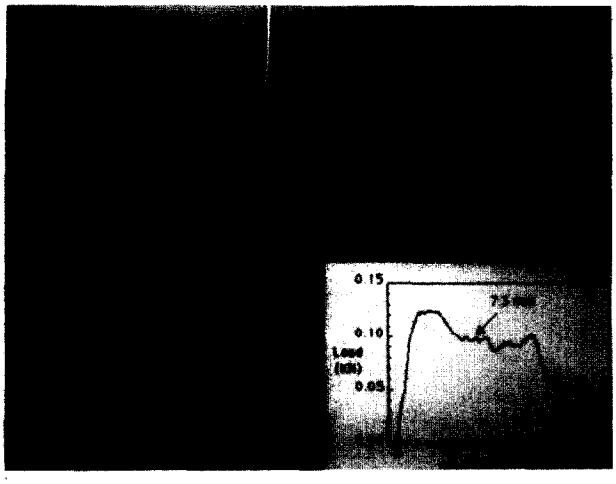

Fig. 7. Digitised image of the same sample at 44 s after test initiation. The corresponding displacement is indicated by an arrow.

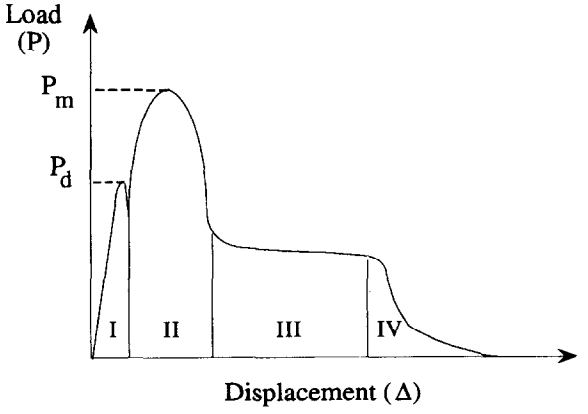

Fig. 9. Typical load–displacement curve for bent fibres. Initial displacement (Region I) enlarged for clarity.

After the fibre was displaced 12·8 mm, the first point of contact exited the matrix and caused a load drop as illustrated in Fig. 8. After this point the load continued to decrease until the whole fibre was removed from the matrix.

The analysis of the video recording and load–displacement curves suggested that a typical pull-out curve from a bent fibre can be divided into four different regions (Fig. 9).

Region I describes the debonding along the fibre/matrix interface for both straight[20–24] and bent fibres. Experimentally the load dropped suddenly after P_d.

After debonding, the fibre begins to slide and Region II corresponds to the removal of the bent section of the fibre from the angled portion of the cement duct. The primary energy dissipation mechanisms are plastic deformation of the steel fibre and friction between the fibre and the porous interfacial texture of the matrix. Observation of the fibres revealed that after debonding the upper surface of the bent fibre was forced against the upper surface of the angled cement duct near the point of the original fibre bend. The pull-out load increased rapidly under small displacements until the reaction force from the cement duct acting on the bent fibre was sufficient to initiate plastic deformation of the steel fibre. It is suggested that prior to the onset of plastic flow, the bent fibre length behaves as a cantilever beam that is anchored at the apex of the fibre bend. The reaction force distributed across the upper fibre surface acts perpendicular to the fibre surface and therefore also serves as the normal force for the friction mechanism. The bending moment at the fixed end of the fibre cantilever increases with increasing pull-out load since the fibre is restricted from upward motion by the constraint of the bent cement duct. A plastic hinge is formed at the bend apex when the bending stress attains the steel fibre yield stress. Only then is the fibre allowed to begin to withdraw from the cement duct. An analytical model of the onset of plastic deformation in Region II will follow the results of planned experiments to measure the distance L_m from the centroid of the distributed reaction bending force to the bend apex as a function of fibre diameter. A plot of experimentally obtained maximum loads from Region II (P_m) as a function of fibre diameter gives straight lines that

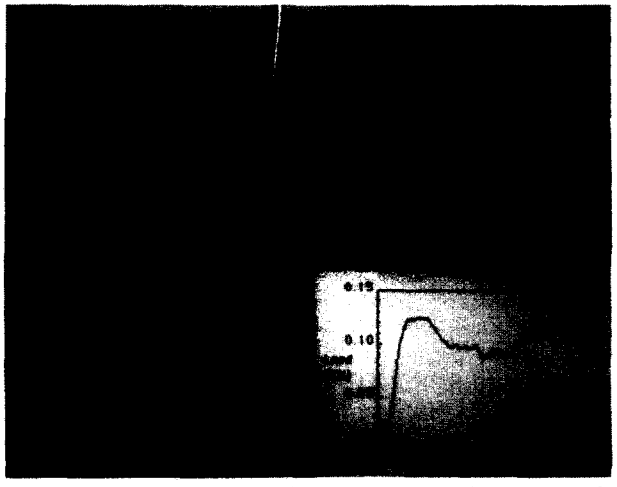

Fig. 8. Digitised image of the same sample at 77 s after test initiation. The corresponding displacement is indicated by an arrow.

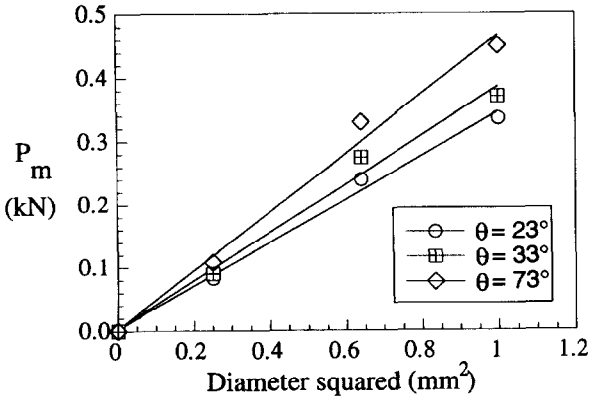

Fig. 10. Experimental maximum load values in Region II as a function of the diameter squared for 90 day water-cured samples.

pass through the origin and increase in slope with increasing bend angle (Fig. 10).

Region III begins when the fibre tip is aligned with the straight cement duct. At this point there is no further plastic deformation but the residual deformation[25] remaining in the fibre from the Region II deformation causes the fibre to contact the duct walls at three points and results in a constant frictional force during Region III pull-out. The pull-out force, P_p, can be modelled as a beam in three point bending, but because of significant damage to the vertical duct walls by the pull-out process, the relationship between fibre diameter and the beam length L_p in this case remains to be determined in planned experiments. A plot of experimentally obtained P_p values versus the square of the fibre diameter again results in straight lines and suggests that L_p may be proportional to the fibre diameter (Fig. 11).

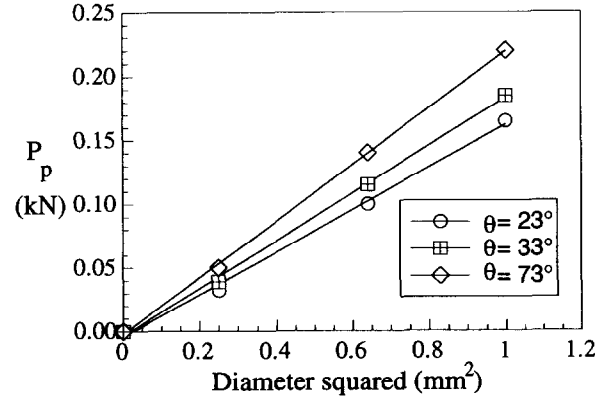

Fig. 11. Experimental plateau load values in Region III as a function of the diameter squared for 90 day water-cured samples.

Region IV corresponds to the removal of the bent fibre section from the cement matrix and the reduction of the frictional pull-out force.

CONCLUSIONS

Video photography of specially prepared samples was used to both observe and correlate the pull-out processes of straight and bent fibres removed from a cement matrix with the significant features of experimentally determined load–displacement curves. The energy dissipation mechanisms governing each stage of the pull-out process included: (1) fibre/matrix debonding, (2) plastic deformation of the fibre and frictional sliding, (3) frictional sliding resulting from residual fibre deformation in Region II, and (4) a sharp reduction in the frictional resistance due to the fibre partially exiting the sample.

Despite the presence of an incorrect position of the fibre due to contact with a smooth glass wall, qualitative mechanics models for the main energy dissipation mechanisms in relation to the main features of the pull-out curve may be suggested. Linear dependence of the maximum and plateau loads for different bend angles with fibre diameter squared was shown.

ACKNOWLEDGEMENTS

The authors thank Mr G. Mocci for helping during the recording of the tests. The financial support of CNR PFEd, SP3 is acknowledged.

REFERENCES

1. Wafa, F. F. & Ashour, S. A., Mechanical properties of high strength fiber reinforced concrete. *ACI Materials Journal*, **89** (1992) 449–55.
2. Beaumont, P. W. R. & Aleszka, J. C., Cracking and toughening of concrete and polymer-concrete dispersed with short steel wires. *Journal of Materials Science*, **13** (1978) 1749–60.
3. Ye, L. & Friedrich, K., Fibre bridging in double cantilever beam specimens and its effect on Mode I interlaminar fracture toughness. *Journal Mater. Sci. Lett.*, **11** (1992) 1537–9.
4. Mindess, S. & Yan, C., Perforation of plain and fibre reinforced concretes subjected to low-velocity impact loading. *Cement and Concrete Research*, **23** (1993) 83–92.
5. Hannant, D. J., *Fibre Cements and Fibre Concretes*. John Wiley, Chichester, 1978.

6. Naaman, A. E. & Najim, H., Bond-slip mechanisms of steel fibers in concrete. *ACI Materials Journal*, **88** (1991) 135–45.
7. Yue, C. Y. & Cheung, W. L., Interfacial properties of fibre-reinforced composites. *Journal of Materials Science*, **27** (1992) 3843–55.
8. Morton, J. & Groves, G. W., Large work of fracture values in wire reinforced, brittle-matrix composites. *Journal of Materials Science*, **10** (1975) 170–2.
9. Soroushian, P. & Bayasi, Z., Fiber type effects on the performance of steel fiber reinforced concrete. *ACI Materials Journal*, **88** (1991) 129–34.
10. Challal, O. & Benmokrane, B., Pullout and bond of glass-fibre rods embedded in concrete and cement grout. *Mater. Struct.*, **26** (1993) 167–75.
11. Banthia, N., Trotter, J. F., Pigeon, M. & Krishnadev, M. R., Deformed steel fiber pullout: material characteristics and metallurgical processes, In *High Performance Fiber Reinforced Cement Composites*, eds. H. W. Remhardt & A. E. Naaman. E. & F. N. Spon, London, RILEM 1992, pp. 456–66.
12. Weiss, H. J., Non-frictional jamming of inclusions — an ignored toughening effect. *Journal of the European Ceramic Society*, **10** (1992) 161–5.
13. Bartos, P. J. M. & Duris, M., Inclined tensile strength of steel fibres in a cement-based composite. *Composites*, **25** (1994) 945–52.
14. Evans, A. G., He, M. Y. & Hutchinson, J. W., Interface debonding and fiber cracking in brittle matrix composites. *J. Am. Ceram. Soc.*, **72** (1989) 2300–03.
15. Gerstle, W. & Ingraffea, A. R., Does bond-slip exist? *Concrete International*, **13** (1991) 44–8.
16. Gent, A. N. & Kaang, S. Y., Pull-out and push-out tests for rubber-to-metal adhesion. *Rubb. Chem. Tech.*, **62** (1991) 757–66.
17. Gent, A. N. & Wang, C., Matrix cracking initiated by fibre breaks in model composite. *Journal of Materials Science*, **27** (1992) 2539–48.
18. Marchese, B. & Marchese, G., Fibre pullout microstructural relationship for cementitious mortars. *J. Mater. Sci. Lett.*, **12** (1993) 1592–5.
19. Bentur, A., Mindess, S. & Diamond, S., Pull-out processes in steel fibre reinforced cement. *Int. J. Cem. Comp. Lightw. Concr.*, **7** (1985) 29–37.
20. Laws, V., Micromechanical aspects of the fibre-cement bond. *Composites*, **13** (1982) 145–51.
21. Zhou, L. M., Kim, J. K. & Mai, Y. W., Interfacial debonding and fiber pull-out stresses. Part II. A new model based on the fracture mechanics approach. *Journal of Materials Science*, **27** (1992) 3155–66.
22. Yue, C. Y. & Cheung, W. L., Interfacial properties of fibrous composites. Part I. Model for debonding and pull-out processes. *Journal of Materials Science*, **27** (1992) 3173–80.
23. Yue, C. Y. & Cheung, W. L., Interfacial properties of fibrous composites. Part II. Determination of interfacial shear strength, interfacial coefficient of friction, and the shrinkage pressure on the fibre. *Journal of Materials Science*, **27** (1992) 3181–91.
24. Li, V. C., Stang, H. & Krenchel, H., Micromechanics of crack bridging in fibre-reinforced concrete. *Mater. Struct.*, **26** (1993) 486–94.
25. Banthia, N. & Pigeon, M., Load relaxation in steel fibres embedded in cement matrices. *Int. J. Cem. Comp. Lightw. Concr.*, **11** (1989) 229–34.